Strojniški vestnik - Journal of Mechanical Engineering 69(2023)5-6, 275-283
DOI:10.5545/sv-jme.2022.423
Original Scientific Paper
Received for review: 2022-10-24
Received revised form: 2023-02-06
Accepted for publication: 2023-03-20


# Wear Behaviour of a Cu-Ni-Sn Hybrid Composite Reinforced with $B_4C$ prepared by Powder Metallurgy Technique

Haiter Lenin Allasi[1,*] – Vettivel Singaravel Chidambaranathan[2] – Mary Vasanthi Soosaimariyan[3]

[1] WOLLO University, Kombolcha Institute of Technology, School of Mechanical and Chemical Engineering, Ethiopia
[2] Chandigarh College of Engineering and Technology, Department of Mechanical Engineering, India
[3] St Xavier's Catholic College of Engineering, Department of Electronics and Communication Engineering, India

*Cu matrix composites benefit from the high electrical and thermal conductivities of Cu and the mechanical wear/erosion resistance of hard reinforcement. In this study, an attempt has been made to determine the effect of the addition of reinforcement $B_4C$ in Cu-Ni-Sn. The $B_4C$ is reinforced to form a hybrid Cu matrix composite with powder metallurgy technique. The hybrid composites are obtained by milling, blending, and compacting the powders to obtain a fine grain-sized particle without aggregation. The grain size and particle nature were characterized using scanning electron microscope (SEM) and X-ray diffraction (XRD) techniques, respectively. The microstructure, density, hardness, and wear rate of the composites were studied. The pin-on-disc method is equipped to study the wear behaviour and coefficient of friction. The sintered density of the prepared Cu-15%Ni is 98.25 %, Cu-8%Sn is 98.20 %, Cu-15%Ni-8%Sn is 98.10 % and Cu-15%Ni-8%Sn-2%$B_4C$ is 95.26 % and lower specific wear rate has been recorded for Cu-15Ni-8Sn-2$B_4C$ 121×10$^{-6}$ mm$^3$/(Nm) and the addition of reinforcement $B_4C$ in Cu-Ni-Sn displays remarkable changes in wear rate and friction coefficient.*

**Keywords: powder metallurgy, copper, wear, characterization, density, composites**

**Highlights**

- *The sintered density of the prepared Cu-15%Ni is 98.25 %, Cu-8%Sn is 98.20 %, Cu-15%Ni-8%Sn is 98.10 % and Cu-15%Ni-8%Sn-2%$B_4C$ is 95.26 %.*
- *The addition of reinforcement $B_4C$ in Cu-Ni-Sn displays remarkable changes in wear rate and friction coefficient.*
- *The lower specific wear rate has been recorded for Cu-15Ni-8Sn-2$B_4C$ is 121×10$^{-6}$ mm$^3$/(Nm).*
- *The severe plastic deformation and cracks are reduced with the addition of $B_4C$.*

## 0 INTRODUCTION

Metal matrix composites (MMCs) are newer materials made in response to increased demand due to emerging applications in the fields of aircraft, space, defence, automotive, and transport because of their good strength and light weight [1] to [4]. The MMCs of different varieties are prepared with powder metallurgy techniques, which is suitable for bulk production. However, due to the existence of residual porosity and exhibited poor mechanical properties, it is used because of its non-wetting behaviour of MMCs.

Cu matrix composites benefit from the high electrical and thermal conductivities of Cu and the mechanical wear/erosion resistance of the reinforcement, such as WC. In addition to Cu–WC, other potential materials for similar applications are Cu– Mo, Cu–$Al_2O_3$, Ag–Mo, Ag–W, Cu-SiC, Cu-TiC, Cu-Sn, Cu-Ni and Ag–CdO [5].

Senthil Kumar et al. studied the tribological behaviours of Cu–6Sn–6Zn–3Pb alloy sliding against AISI 321 stainless steel under sea water, distilled water and dry sliding conditions are studied on a pin-on-disc tester. Generally, the friction coefficient in distilled water is the largest and the smallest in dry sliding. The wear mechanism is a micro-plough and plastic deformation in distilled water and under dry sliding [6].

Vettivel et al. studied the development of Cu-reinforced SiC particulate composites; SiC particles as reinforcement were blended with unmilled and as-milled Cu powder with reinforcement contents of 10 vol. %, 20 vol. %, 30 vol. %, and 40 vol. % using powder metallurgy. X-ray diffraction of all the composites was done in order to determine the various phases in the composites. Scanning electron microscopy (SEM) and EDS (electron diffraction X-ray spectroscopy) were carried out for the microstructure analysis of the composites. Cu-SiC composites containing higher vol. % of the SiC show better wear resistance [7].

The microstructure and tensile properties of Cu alloy reinforced with boron carbide ($B_4C$) using a stir-casting technique. The hardness of the composites increased gradually by adding the reinforcement compared to the base alloy properties. The yield strength also increases by adding the $B_4C$ particulates into the Cu alloy matrix [8]. Another study confirmed that mechanical and thermal properties of multi-

*Corr. Author's Address: Wollo University, Kombolcha Institute of Technology, School of Mechanical and Chemical Engineering, Ethiopia, drahlenin@kiot.edu.et

walled carbon nanotubes (CNT) reinforced Cu–10Sn alloy composites. Microstructural observations showed that CNTs were retained in the composite matrix after laser processing. The addition of CNTs showed improvement in strain hardening, mechanical, and thermal properties of Cu–10Sn alloy. Composites with 12 vol. % CNTs showed more than an 80 % increase in the Young's modulus and a 40 % increase in the thermal conductivity of Cu–10Sn alloy **[9]** and **[10]**.

Cu is used as a primary matrix and Ni and Sn as a secondary matrix and 2 % $B_4C$ as reinforcement added to the alloy (Cu-15%Ni-8%Sn). These spindle alloys cover excellent bearing properties and are thus used in a wide range of applications **[11]**. Copper an electrolytic ally processed and precipitated metal is taken and coated with nickel and tin with volume fractions of 15 % and 8 % respectively. Nickel is compatible and provides better reinforcement and adhesion to the carbide materials **[12]**.

In this study, copper, nickel, tin and boron carbide are reinforced to form hybrid MMCs via a powder metallurgy technique. The hybrid composites are obtained by milling, blending, and compacting powders to obtain a fine grain-sized particle without aggregation. The effect of the addition of $B_4C$ in mechanical and tribological behaviour has been studied.

## 1 METHODS

Electrolytic copper powder with density 8.92 g/cm$^3$ at 20 ºC, nickel with 8.9 g/cm$^3$ at 20 ºC and tin with 7.3 g/cm$^3$ at 20 ºC, whereas boron carbide 2.52 g/cm$^3$ at 20 ºC is reinforced to the metals. These are mechanically alloyed to the micron range and the samples are fabricated with a powder metallurgy technique to prepare MMCs. Then, the obtained MMC is sintered to high temperature of about 900 ºC. The sintered density of the Cu-15%Ni is 98.25 %, Cu-8%Sn is 98.20 %, Cu-15%Ni-8%Sn is 98.10 % and Cu-15%Ni-8%Sn-2%$B_4C$ is 95.26 %.

The morphology and size of the particles are examined for individual metals and alloys, also after

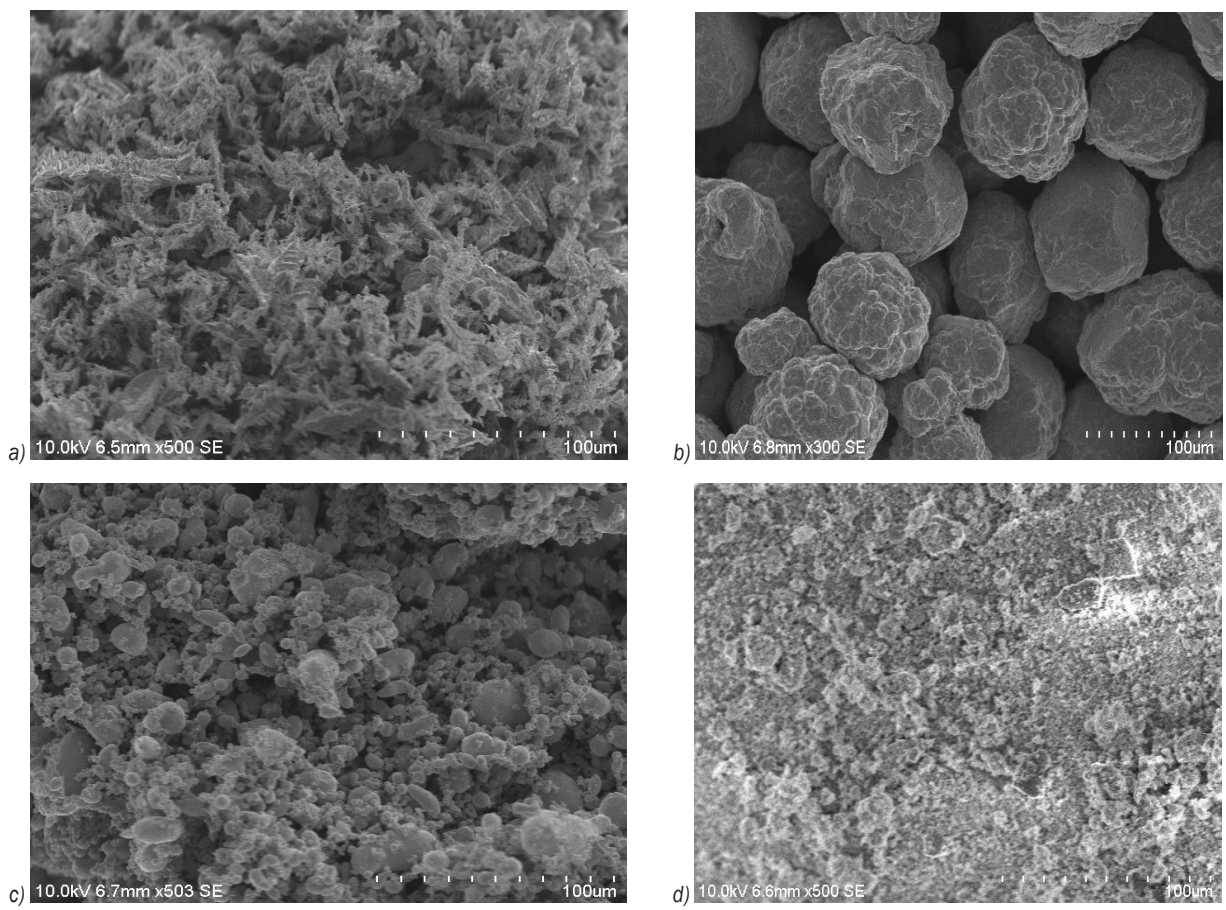


**Fig. 1.** *SEM image of unreinforced materials: a) Copper (Cu), b) Nickel (Ni), c) Tin (Sn, and d) 2% Boron carbide (B4C)*

reinforcement added to the materials (i.e., MMC using SEM). The crystal structure and the phase change of the materials are studied using an X-ray diffractometer (XRD) with respect to the intensity peaks and materials diffraction angle $2\theta$. The hardness, strength and wear of the composites are determined using a pin-on-disc apparatus with which the sliding distance, sliding velocity, load, and speed are applied to the composites by varying these parameters.

The SEM image shows the particle sizes are 100 µm, 30 µm, 20 µm, and 10 µm for all metals such as Cu, Ni, Sn and $B_4C$, respectively. The MMCs Cu-15%Ni, Cu-8%Sn, Cu-15%Ni-8%Sn and Cu-15%Ni-8%Sn-2%$B_4C$ also exhibit smaller sizes. The morphology and grain nature of the materials are visualized using SEM and are obtained in different morphological forms. The Cu metal looks like cylindrical short tubes and have a slightly adhesive nature, whereas Ni, Sn and $B_4C$ show solid spherical balls with much less agglomeration.

The mixed MMCs after 2 % $B_4C$ is reinforced exhibit good morphology and fine-grain nature. Fig. 2a and b show the SEM images of Cu and Ni, respectively. and the diameter of the particles ranges from 5 µm to 20 µm, whereas Fig. 2c and d exhibit foamy and short fibrous materials, respectively. The MMC of Cu-15%Ni-8%Sn-2%$B_4C$ exhibits improved shape, with cylindrical tubes and spherical balls compressed against one another more evenly and resembling a very fine dispersion of particles with diameters ranging from 1 µm to 10 µm. The composites are well mixed, while the powders are crushed and blended to obtain good compaction of materials.

The X-ray diffractometer analysis of the particles in Fig. 3 reveals good crystal structure and phase development in the lattice fringes. Cu and Ni have a peak that corresponds to the (111) hkl lattice plane (Fig. 2a and b) and shows pure materials that have not been reacted with by the atmosphere, but Sn and $B_4C$ have illogical peaks that show fewer impurities. For Sn and $B_4C$, the hkl lattice planes are 200 and 024, respectively, due to the amorphous nature of the particles.

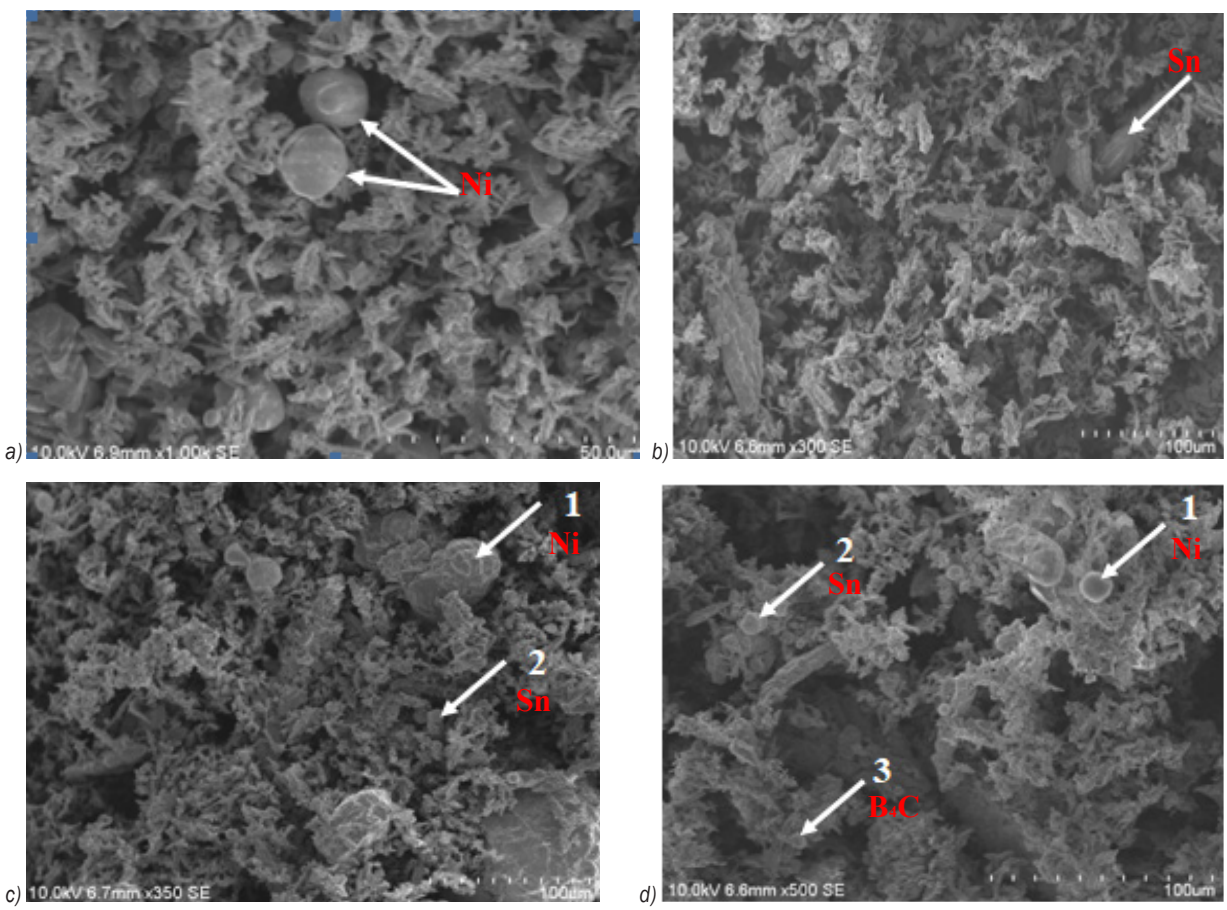


**Fig. 2.** *SEM images of reinforced materials; a) Cu-Ni, b) Cu-Sn, c) Cu-Ni-Sn, and d) Cu-Ni-Sn-2%B4C*

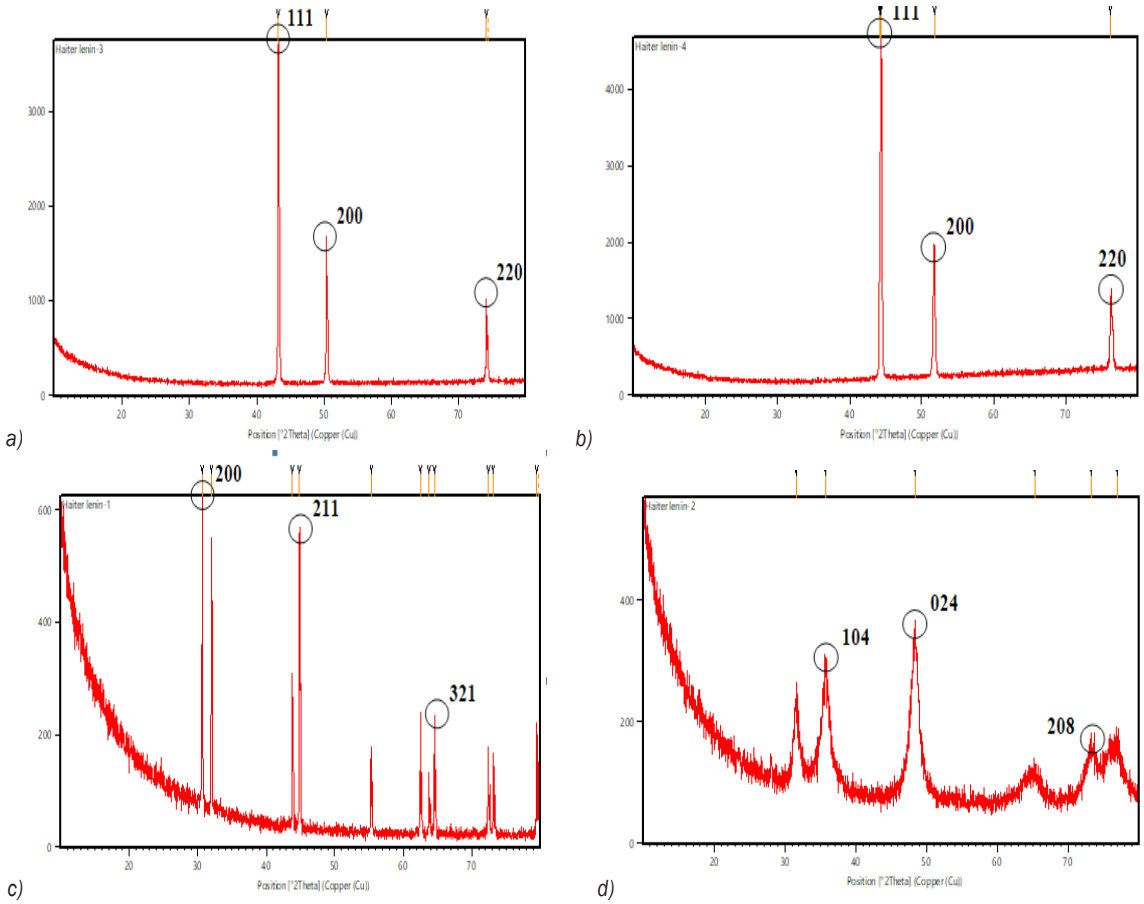


**Fig. 3.** *XRD patterns for unreinforced materials; a) Copper (Cu), b) Nickel (Ni), c) Tin (Sn, and d) Boron carbide ($B_4C$)*

The materials have incorporated each other into copper metal and then $B_4C$ is reinforced to the composites and the composites are structurally characterized by XRD, which explores the hkl lattice planes with respect to the intensities and $2\theta$ shown in Fig. 4. The materials are produced by mechanically alloying and composites are fabricated by Powder Metallurgy PM technique, milled, crushed, and then blended. Finally, the compaction of the material is well fitted by uniform dispersion of particles and sintered to a high temperature of about 900 ºC to avoid further grain growth. Thus, the lattice parameters of the composites are uniformly distributed for Cu-Ni, Cu-Sn and Cu-Ni-Sn. While the reinforced composites contain carbon particles ($B_4C$), the peaks point at another $2\theta$ position and all other materials represent peaks in the same $2\theta$ position.

### 2.1 Wear test

The pin-on-disc instrument is equipped to study the hardness and wear rate of the composites. Ultra-hard materials are used for wear-resistant applications because they have good sliding interaction with the abrasive particles [13]. This research describes the wear rate of metals Cu, Ni and Sn individually and then alloy Cu-Ni-Sn and also for MMCs Cu-Ni-Sn-$B_4C$, which exhibits better resistance to wear compared to alloy. The wear rate varies according to the variable parameters and contribution of the materials volume concentration.

The specific wear rates of the unreinforced and reinforced composites are analysed by changing the process parameters, mainly weight percentage or volume concentration, sintering temperature, load, sliding distance, sliding velocity, friction coefficient and volume loss of the composite material. Vettivel et al. [14], analysed the friction coefficient and specific wear rate by ANOVA (Analysis of Variance) method and found that the result mainly depends on the type and size of the reinforcement phase of the particles. Also, the metal-on-metal contact that takes place at the initial stage is relatively low at the steady state [15].

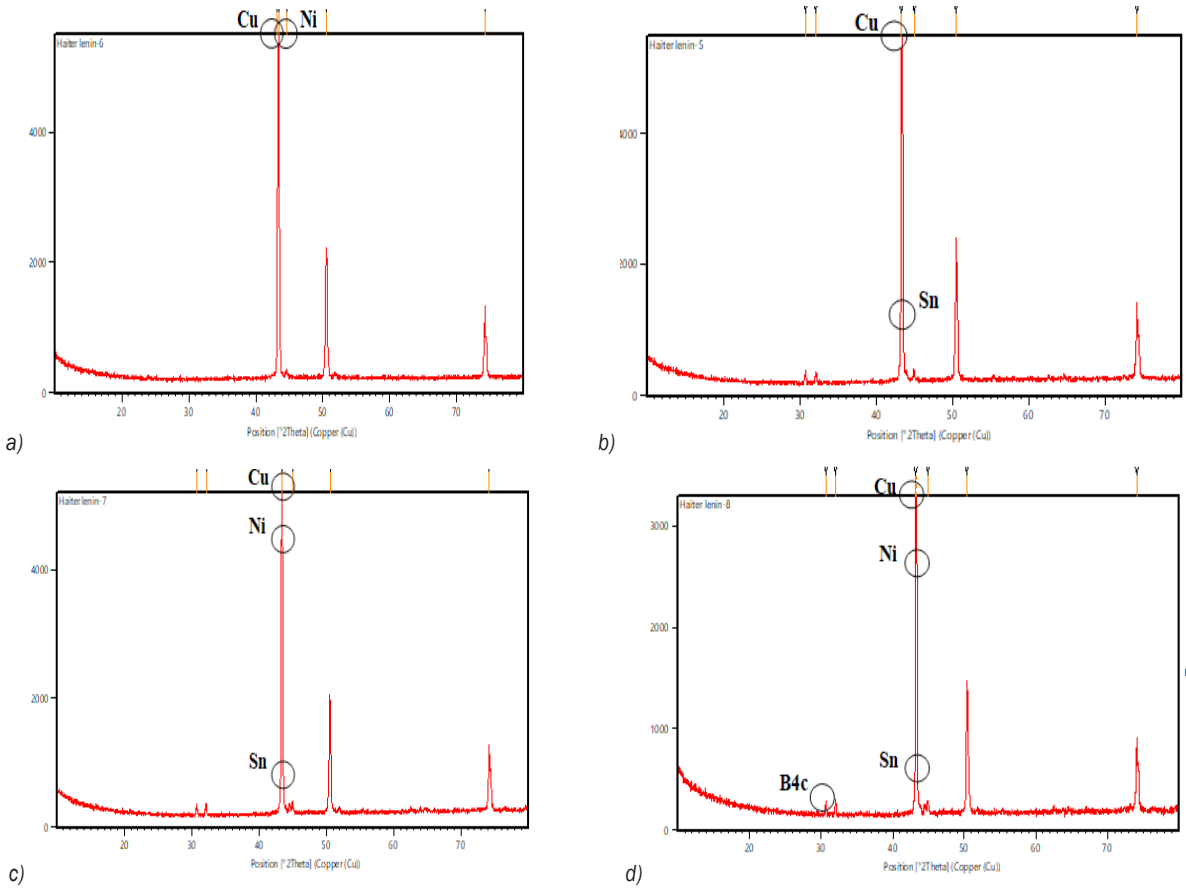


**Fig. 4.** *XRD patterns of reinforced composites; a) Cu-Ni, b) Cu-Sn, c) Cu-Ni-Sn, and d) Cu-Ni-Sn-2%$B_4C$*

## 2 RESULTS AND DISCUSSION

### 2.1 Effect of Sliding Distance on Specific Wear Rate

Fig. 5 represents the specific wear rate increases with the sliding distance significantly. There is a gradual and linear raise in specific wear rate due to the hardness of the composites according to the constituents added to it **[16]** to **[18]**. From Fig. 5a, pure copper metal is tested for a specific wear rate, which shows $78\times10^{-5}$ mm$^3$/(Nm) to $340\times10^{-6}$ mm$^3$/(Nm), at a constant sintering temperature of 900 ºC and sliding speed 20.94 m/s and variable parameters like sliding distance and load applied is 400 m to 1000 m and 10 N to 25 N, correspondingly. Also, a specific wear rate is experienced for alloy Cu-15Ni and Cu-8Sn, which reveals that $130\times10^{-6}$ mm$^3$/(Nm), also for Cu-15Ni-8Sn alloy shows $127\times10^{-6}$ mm$^3$/(Nm) with that a constant temperature and sliding speed and variable parameters of sliding distance at 1000 m and load applied of about 25 N. Here, we can infer that the alloy can have the intense effect in specific wear rate compared to pure metal, which is at very heavy loading and high sliding distance. If the reinforcement $B_4C$ is added to that matrix alloy, the composite Cu-15Ni-8Sn-2$B_4C$ exhibits a reduced wear rate of about $121\times10^{-6}$ mm$^3$/Nm. In this work, only 2%$B_4C$ is added as reinforcement resulted with a good reduction in specific wear rate compared to metal and matrix alloy. The lower specific wear rate has been recorded for Cu-15Ni-8Sn-2$B_4C$. The decrement in specific wear rate is due to the addition of $B_4C$ in the Cu-15Ni-8Sn. The results are in good agreement with other studies **[9]** and **[14]**.

### 2.2 Worn Surface and Microstructure

The worn surface analysis of the MMCs in various volume fractions was investigated using SEM. The samples were tested by placing it in a holder inside the vacuum chamber. The image displayed information about the composites after the load was applied to it. Along the sliding direction, the materials withstand and prevent deformation and formation of oxide

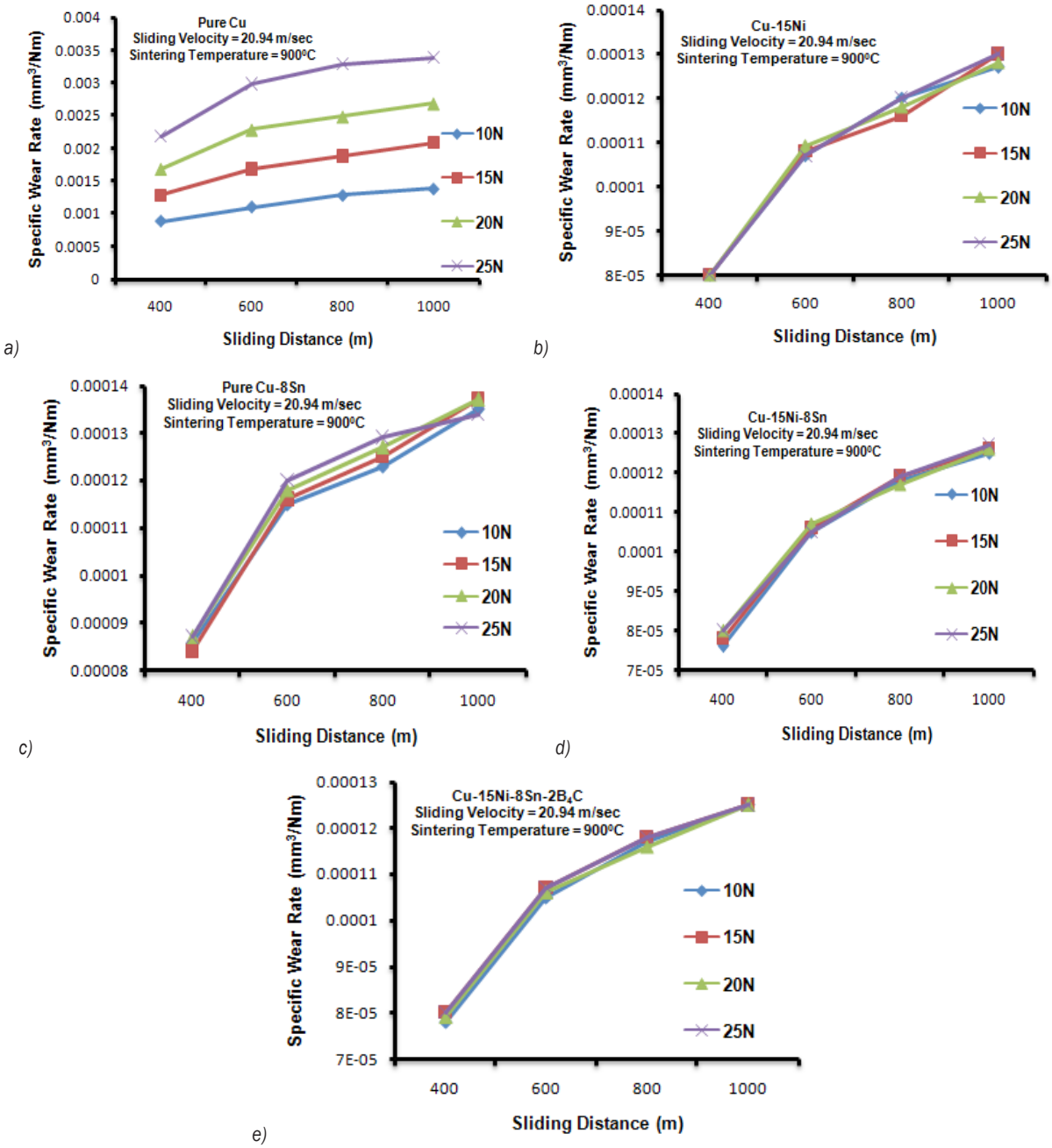


**Fig. 5.** *The effect of sliding distance on specific wear rate of metal, matrix and composites; a) Cu, b) Cu-15Ni, c) Cu-8Sn, d) Cu-15Ni-8Sn, e) Cu-15Ni-8Sn-2B$_4$C*

debris at the interface region or at the contact surface; thus grooves, shear wedges, depth of penetration to wear, ploughing, and cracks can be observed. Due to the wear, the materials are abraded [19].

The worn surface of the unreinforced specimen is caused by the removal of material from the surface during the wear test. To avoid the rolling of the specimen, during the test the material was held in the testing machine [20]. Ling. et al. [20] analysed the microstructure nature of the Al-SiC composites; they found that while adding reinforcement to the matrix, big pores were found, due to the low volume fraction and grain size of the reinforcement added to the composites [21]. The particles are in heterogeneous distribution and are so large that the worn surface can be seen; the durable bonding between the

reinforcement and matrix resulted in particle accumulation and grain boundaries [22] and [23].

The worn surface of the unreinforced Cu at constant load and wearing time is shown in Fig. 6a, it has long smooth patches consisting of cracks and wear grooves. At the centre of the specimen, long shear wedges can be seen. Copper shows short and discontinuous pitting steps because of the unreinforced and heterogeneous distribution of particles with irregular size. From Fig. 6b and c, it can be inferred that Cu-Ni and Cu-Sn are unreinforced; the worn surface can be seen with shear wedges and wear grooves. Fig. 6d shows matrix alloy Cu-15Ni-8Sn exhibiting wear at constant load, time and sliding direction. Here also carbide material is not reinforced with this matrix and exhibits long and continuous smooth patches, cracks, and reduced wear grooves; it can withstand stress at high temperatures. Fig. 6e shows the morphology of the worn surface of the composite (reinforcement of carbide materials) Cu-15Ni-8Sn-2$B_4C$ at constant load and time. The wear occurs according to the sliding direction and has

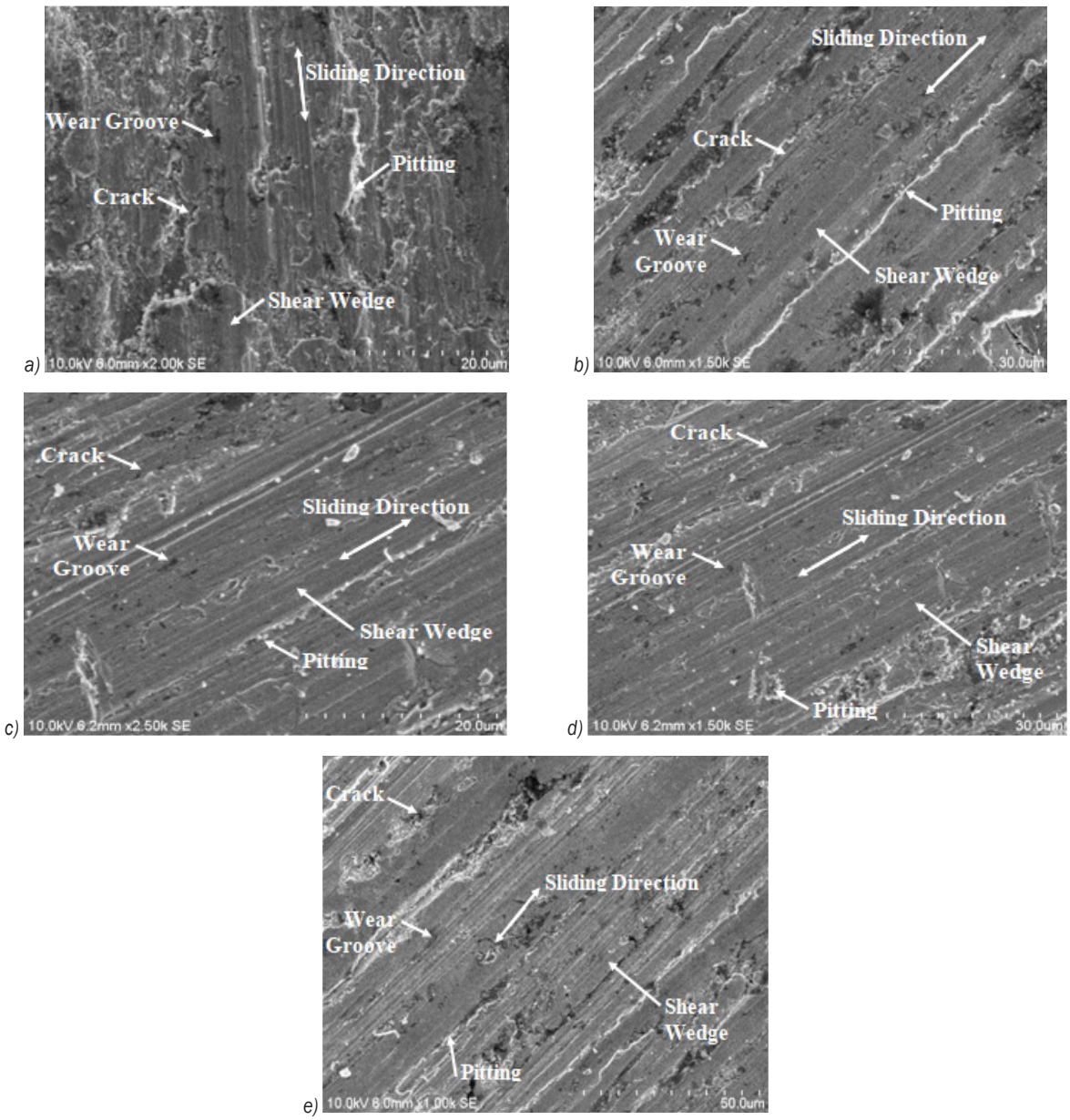


**Fig. 6.** *SEM image of worn surface for unreinforced and reinforced composites; a) Cu-Ni, b) Cu-15Ni, c) Cu-8Sn, d) Cu-15Ni-8Sn, and e) Cu-15Ni-8Sn-2$B_4C$*

rough patches with large amounts of wear grooves compared to unreinforced material and matrix alloy. The morphology clearly infers that cracks are fewer, and pitting is continuous with long shear wedges and so it withstands wear resistance, and the surface is not damaged while increasing the temperature. The composite after reinforcing with $B_4C$ with less volume fraction at 2 % resulted in a negative effect on the wear of the material and provided hardness and strength to the composite.

### 2.2 Sintered Density Test

Sintering is the principal factor for controlling the density of the composite materials; sintering time and temperature play major roles. When there is a huge variation in load and temperature, the density affects extensively [17]. The increase in experimental density is a consequence of enhancing the mechanical property of the specimen. The higher the density, the better the strength of the composites; this is because the reduced size of pores reduces the defect of the material.

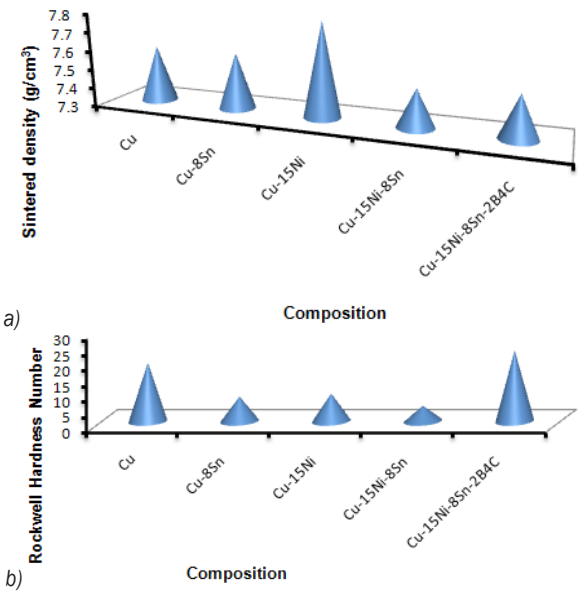


**Fig. 7.** *Effect of composition on: a) sintered density, and b) hardness*

In this work, the performance of the composite is good, but the experimental density is less for MMC Cu-15Ni-8Sn-2$B_4C$. Here, the contribution of carbide is less (volume fraction 2 %), but the copper matrix contribution is normal, so better in other performances and meagre in experimental density. The bar plot shown in Fig. 7a represent the effect of sintered density at 900 °C. The unreinforced copper and Cu-8Sn show approximately 7.6 g/cm³ density. The matrix Cu-15Ni display 7.8 g/cm³, while the metal matrix and composite (Cu-15Ni-8Sn and Cu-15Ni-8Sn-2$B_4C$) are at 7.5 g/cm³ and 7.52 g/cm³ respectively. From this, we can infer that the higher the weight fraction, the better the density of the material.

### 2.3 Hardness Test

The Rockwell hardness is a test method, and ASTM E-18 is the commonly used method to be equipped. The hardness is determined with the help of an indenter present in equipment that measures the size of impression and depth of penetration of the indenter, performed by the composite material at the surface of the material to be loaded for testing. The Rockwell hardness test method is more accurate than other types of testing methods and is used for all metals and composites.

The present study investigated integrated the various compositions and tested for hardness and found the Rockwell hardness number. The material is heated to a sintering temperature of 900 ºC, the powders were compacted, and the load is applied to it. Based on the hardness of the material, it withstands the load.. From Fig 7b, hardness number is high for the reinforced material. Even though, the addition of boron carbide volume fraction is less, the hardness of the composite is enhanced. The Rockwell hardness number of the unreinforced Cu-15Ni-8Sn and MMC Cu-15Ni-8Sn-2B4C is 5 and 23, respectively.

## 3 CONCLUSIONS

The unreinforced copper, Cu-Ni, Cu-Sn and Cu-Ni-Sn-B4C composites were prepared using the powder metallurgy technique. The morphology, grain size and uniform dispersion of the composites were characterized using SEM and XRD. The tribological, hardness and density of the specimens were tested, and the following conclusions are drawn.

- The SEM images confirm that the Sn, Ni and $B_4C$ particles are distributed uniformly throughout the matrix.
- The sintered density of the prepared Cu-15%Ni is 98.25 %, Cu-8%Sn is 98.20 %, Cu-15%Ni-8%Sn is 98.10 % and Cu-15%Ni-8%Sn-2%$B_4C$ is 95.26 %
- Cu-15Ni-8Sn-2$B_4C$ exhibits lower wear rate of about $121\times10^{-6}$ mm³/(Nm) compared to the other prepared samples. It is mainly due to the nature and the addition of hard reinforcement $B_4C$ in the Cu-15Ni-8Sn.

- Worn surface confirmed that there is a reduction of plastic deformation and cracks due to the addition of B4C.

## 5 REFERENCES


[1] Karthikeyan, G., Jinu, G. R. (2016). Dry sliding wear behavior optimization of stir cast LM6/ZrO2 composites by response surface methodology analysis. *Transactions of the Canadian Society for Mechanical Engineering*, vol. 40, no. 3, p. 351-369, **DOI:10.1139/tcsme-2016-0026**.

[2] Palanikumar, K., Karthikeyan, R. (2007). Assessment of factors influencing surface roughness on the machining of Al/SiC particulate composites. *Materials & Design*, vol. 28, no. 5, p. 1584-1591, **DOI:10.1016/j.matdes.2006.02.010**.

[3] Moustafa, S.F., Abdel-Hamid, Z., Abd-Elhay, A. M. (2002). Copper matrix SiC and Al2O3 particulate composites by powder metallurgy technique. *Materials Letters*, vol. 53, no. 4-5, p. 244-249, **DOI:10.1016/S0167-577X(01)00485-2**.

[4] Kaczmar, J.W., Pietrzak, K., Włosiński, W. (2000). The production and application of metal matrix composite materials. *Journal of Materials Processing Technology*, vol. 106, no. 1-3, p. 58-67, **DOI:10.1016/S0924-0136(00)00639-7**.

[5] Singh, J.B., Cai, W., Bellon, P. (2007). Dry sliding of Cu-15 wt% Ni-8 wt% Sn bronze: Wear behaviour and microstructures. *Wear*, vol. 263, no. 1-6, p. 830-841, **DOI:10.1016/j.wear.2007.01.061**.

[6] Narayanasamy, P., Balaji, A.N., Vettivel, S.C. (2018). Microstructural, electrical, thermal and tribological studies of copper-fly ash composites through powder metallurgy. *Bulletin of the Polish Academy of Sciences: Technical Sciences*, vol. 66, no. 6, p. 935-940, **DOI:10.24425/bpas.2018.125941**.

[7] Senthil Kumar, P., Manisekar, K., Vettivel, S.C. (2016). Effect of extrusion on the microstructure and tribological behavior of copper-tin composites containing $MoS_2$. *Tribology Transactions*, vol. 59, no. 6, p. 1016-1030, **DOI:10.1080/10402004.2015.1131347**.

[8] Vettivel, S.C., Selvakumar, N., Ponraj, N.V. (2013). Tribological behaviour of Cu-5W sintered powder composite. *Advanced Materials Research*, vol. 622, p. 1300-1304, **DOI:10.4028/www.scientific.net/AMR.622-623.1300**.

[9] Ponraj, N.V., Azhagurajan, A., Vettivel, S.C., Sahaya Shajan, X., Nabhiraj, P.Y., Haiterlenin, A. (2019). Modeling and optimization of the effect of sintering parameters on the hardness of copper/graphene nanosheet composites by response surface methodology. *Metal Science and Heat Treatment*, vol. 60, p. 611-615, **DOI:10.1007/s11041-019-00327-z**.

[10] Vijay Ponraj, N., Azhagurajan, A., Vettivel, S.C., Sahaya Shajan, X., Nabhiraj, P.Y. (2018). Study of processing and microstructure of copper composite reinforced with graphene nanosheet by powder metallurgy technique. *Powder Metallurgy and Metal Ceramics*, vol. 56, p. 523-534, **DOI:10.1007/s11106-018-9925-9**.

[11] Manohar, G., Dey, A., Pandey, K.M., Maity, S. R. (2018). Fabrication of metal matrix composites by powder metallurgy: A review. *AIP Conference Proceedings*, vol. 1952, no. 1, art. ID 020041, **DOI:10.1063/1.5032003**.

[12] Meignanamoorthy, M., Ravichandran, M. (2018). Synthesis of metal matrix composites via powder metallurgy route: a review. *Mechanics and Mechanical Engineering*, vol. 22, no. 1, p. 65-76, **DOI:10.2478/mme-2018-0007**.

[13] Lieblich, M., Corrochano, J., Ibáñez, J., Vadillo, V., Walker, J.C., Rainforth, W.M. (2014). Subsurface modifications in powder metallurgy aluminium alloy composites reinforced with intermetallic $MoSi_2$ particles under dry sliding wear. *Wear*, vol. 309, no. 1-2, p. 126-133, **DOI:10.1016/j.wear.2013.11.012**.

[14] Vettivel, S.C., Selvakumar, N., Narayanasamy, R., Leema, N. (2013). Numerical modelling, prediction of Cu-W nano powder composite in dry sliding wear condition using response surface methodology. *Materials & Design*, vol. 50, p. 977-996, **DOI:10.1016/j.matdes.2013.03.072**.

[15] Johnyjames, S., Annamalai, A.R. (2017). Fabrication of aluminium metal matrix composite and testing of its property. *Mechanics, Materials Science & Engineering*, vol. 9, **DOI:10.2412/mmse.62.86.695**.

[16] Kumar, T.R., Swamy, R.P., Chandrashekar, T.K. (2013). An experimental investigation on wear test parameters of metal matrix composites using Taguchi technique. *Indian Journal of Engineering and Materials Sciences*, vol. 20, p. 329-333

[17] Radhika, N., Sasikumar, J., Jojith, R. (2021). Effect of grain modifier on mechanical and tribological properties of al-si alloy and composite. *Silicon*, vol. 13, p. 841-855, **DOI:10.1007/s12633-020-00476-4**.

[18] Cao, F., Chen, C., Wang, Z., Muthuramalingam, T., Anbuchezhiyan, G. (2019). Effects of silicon carbide and tungsten carbide in Aluminium metal matrix composites. *Silicon*, vol. 11, p. 2625-2632, **DOI:10.1007/s12633-018-0051-6**.

[19] Kumar, C.R., Malarvannan, R.R.R., JaiGanesh, V. (2020). Role of SiC on mechanical, Tribological and thermal expansion characteristics of B4C/Talc-reinforced Al-6061 hybrid composite. *Silicon*, vol. 12, p. 1491-1500, **DOI:10.1007/s12633-019-00243-0**.

[20] Ling, G., Shui, Z., Sun, T., Gao, X., Wang, Y., Sun, Y., Wang, G., Li, Z. (2018). Rheological behavior and microstructure characteristics of SCC incorporating metakaolin and silica fume. *Materials*, vol. 11, no. 12, art. ID 2576, **DOI:10.3390/ma11122576**.

[21] Tjong, S.C., Lau, K.C. (2000). Abrasive wear behavior of TiB2 particle-reinforced copper matrix composites. *Materials Science and Engineering: A*, vol. 282, no. 1-2, p. 183-186, **DOI:10.1016/S0921-5093(99)00752-2**.

[22] Öksüz, K.E. (2015). A study on Al2O3/SiC/B4C reinforced Cu-Sn matrix composite by warm compaction powder metallurgy. *Advanced Materials Research*, vol. 1128, p. 123-126, **DOI:10.4028/www.scientific.net/AMR.1128.123**.

[23] Saminatharaja, D., Periyakgounder, S., Selvaraj, M., Elangandhi, J. (2021). Performance study of EDM process parameters using $TiC/ZrSiO_4$ particulate-reinforced copper composite electrode. *Strojniški vestnik - Journal of Mechanical Engineering*, vol. 67, no. 11, p. 547-556, **DOI:10.5545/sv-jme.2021.7254**.